Statistical Study of the Interplanetary Coronal Mass Ejections from 1995 to 2015

Yutian Chi, Chenglong Shen, Yuming Wang, Mengjiao Xu, Pinzhong Ye & Shui Wang

Solar Physics
A Journal for Solar and Solar-Stellar Research and the Study of Solar Terrestrial Physics

ISSN 0038-0938
Volume 291
Number 8

Sol Phys (2016) 291:2419-2439
DOI 10.1007/s11207-016-0971-5

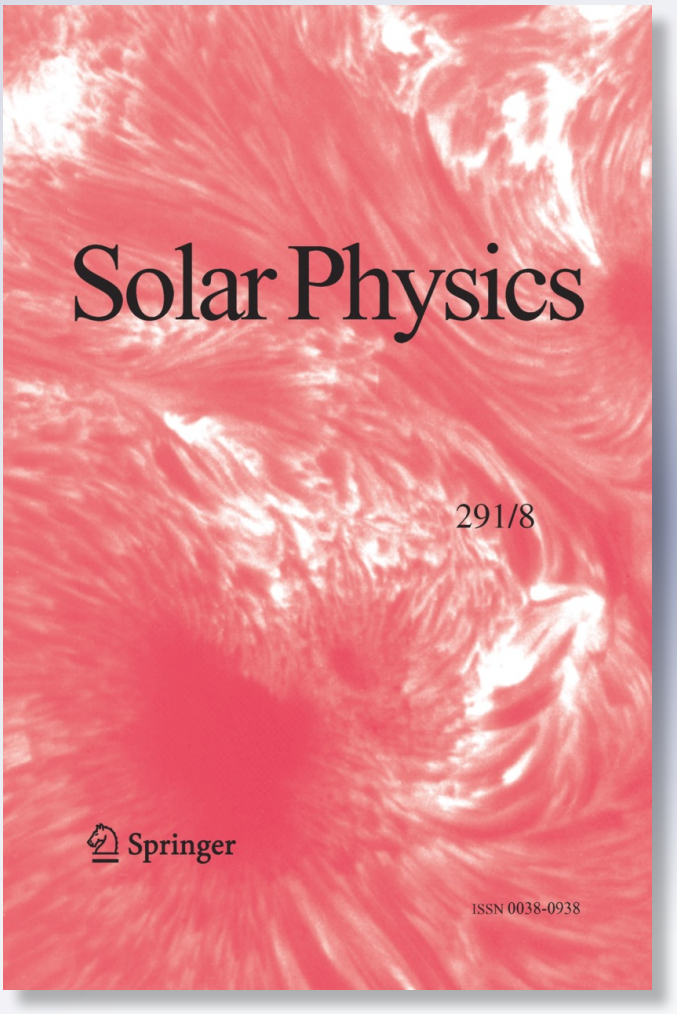

Springer

Solar Phys (2016) 291:2419–2439
DOI 10.1007/s11207-016-0971-5

Statistical Study of the Interplanetary Coronal Mass Ejections from 1995 to 2015

Yutian Chi[1,2] · Chenglong Shen[1,3] · Yuming Wang[1,4] · Mengjiao Xu[1] · Pinzhong Ye[1] · Shui Wang[1,5]

Received: 2 May 2015 / Accepted: 8 August 2016 / Published online: 22 September 2016

Abstract We establish a catalog of interplanetary coronal mass ejections (ICMEs) during the period from 1995 to 2015 using the *in-situ* observations from the *Wind* and ACE spacecraft. Based on this catalog, we extend the statistical properties of ICMEs to the maximum phase of Solar Cycle 24. We confirm previous results that the yearly occurrence frequencies of ICMEs and shocks, the ratios of ICMEs driving shocks are correlated with the sunspot numbers. For the magnetic cloud (MC), we confirm that the yearly occurrence frequencies of MCs do not show any correlation with sunspot numbers. The highest MC ratio of ICME occurred near the solar minimum. In addition, we analyzed the yearly variation of the ICME parameters. We found that the ICME velocities, the magnetic-field strength, and their related parameters are varied in pace with solar-cycle variation. At the solar maximum, ICMEs move faster and carry a stronger magnetic field. By comparing the parameters between MCs and non-MC ejecta, we confirm the result that the magnetic-field intensities of MC are higher than those in non-MC ejecta. Furthermore, we also discuss the forward shocks driven by ICMEs. We find that one half of the ICMEs have upstream shocks and ICMEs with shocks have faster speed and higher magnetic-field strength than the ICMEs without shocks. The magnetic-field parameters and solar-wind plasma parameters in the shock sheath regions are higher than those in the ejecta regions of ICMEs from a statistical point of view.

Keywords ICME · MC · Shock · Sheath region

✉ C. Shen
clshen@ustc.edu.cn

1 CAS Key Laboratory of Geospace Environment, Department of Geophysics and Planetary Sciences, University of Science & Technology of China, Hefei, Anhui 230026, China

2 Sate Key Laboratory of Space Weather, Chinese Academy of Sciences, Beijing 100190, China

3 Synergetic Innovation Center of Quantum Information & Quantum Physics, University of Science and Technology of China, Hefei, Anhui 230026, China

4 Collaborative Innovation Center of Astronautical Science and Technology, Hefei, Anhui, China

5 Mengcheng National Geophysical Observatory, School of Earth & Space Sciences, University of Science & Technology of China, Hefei, China

1. Introduction

Interplanetary coronal mass ejections (ICMEs), which are thought to be the interplanetary counterparts of coronal mass ejections (CMEs), have been reported and studied by *in-situ* measurements for decades (*e.g.* Gosling, Pizzo, and Bame, 1973; Burlaga *et al.*, 1981, 2001; Cane and Richardson, 2003a; Jian *et al.*, 2006; Wimmer-Schweingruber *et al.*, 2006; Gopalswamy, 2006; Kilpua *et al.*, 2009; Richardson and Cane, 2010; Jian, Russell, and Luhmann, 2011; Kilpua *et al.*, 2012, 2014 and references therein). As the important carrier of the south component of the interplanetary magnetic field (IMF), ICMEs are thought to be the main sources of the geomagnetic storms, especially the intense geomagnetic storms. (*e.g.* Xue *et al.*, 2005; Yermolaev and Yermolaev, 2006; Gopalswamy, 2006; Gonzalez *et al.*, 2007, 2011; Zhang *et al.*, 2007; Echer, Gonzalez, and Tsurutani, 2008; Wu *et al.*, 2013).

However, there is no clear consensus on what the ICME individual characteristics are from solar wind *in-situ* observation. ICMEs may lose their characteristics during the propagation, as a result of interaction between CMEs and other structures (such as the heliosphere current sheet (HCS)). There are various signatures of ICMEs based on *in-situ* solar-wind observations (*e.g.* Zurbuchen and Richardson, 2006, Wu and Lepping, 2011 and references therein). Wu and Lepping (2011) summarized 12 different physical entities to identify the existence of an ICME. The 12 potentially applicable quantities are i) enhanced magnetic-field intensity, ii) smoothly changing field direction, iii) relatively low proton temperature, iv) low proton plasma β, v) bidirectional streaming of electrons, vi) bidirectional streaming of low energy protons, vii) high charge states of ions and compositional signatures, viii) low charge states, ix) singly charged He^{+}, x) bidirectional particle flows at cosmic-ray energies (1 MeV), xi) bidirectional solar-wind electron heat flux events (BDEs), xii) including ground-based data, the occurrence of a one- or two-step Forbush decreases (see Wu and Lepping, 2011 and references therein). In addition, the declining velocity profile which indicates the expansion of ICMEs also should be used as a signature to identify the ICME (*e.g.* Zurbuchen and Richardson, 2006, Jian *et al.*, 2006 and references therein). It should be noted that, none of these signatures can be observed in all ICMEs. Thus, different authors used different criteria to identify ICMEs and their related structures from *in-situ* observations (*e.g.* Wang *et al.*, 2002; Jian *et al.*, 2006; Lepping *et al.*, 2006a; Richardson and Cane, 2010; Kilpua *et al.*, 2012; Wu and Lepping, 2015 and references therein).

The magnetic cloud (MC), which is thought to be a special type of ICME, shows a region of high magnetic-field strength compared to its surroundings, low proton temperature, low proton β, and a smoothly changing (rotating) magnetic-field direction (*e.g.* Burlaga *et al.*, 1981; Burlaga, 1988; Klein and Burlaga, 1982). Early studies showed that around 30 % (Gosling, 1990; Wu and Lepping, 2007) to 50 % (Cane, Richardson, and Wibberenz, 1997) of ICMEs at one AU exhibited magnetic-flux ropes and could be described as a force-free cylindrical magnetic-flux tube. After that, different methods were developed to fit the MCs (*e.g.* Lepping, Jones, and Burlaga, 1990; Hau and Sonnerup, 1999; Hu and Sonnerup, 2001, 2002; Möstl *et al.*, 2010; Wang *et al.*, 2015 and references therein). Recently, using an MC fitting method, Lepping *et al.* (2006a, 2011, 2015) compiled an MC catalog automatically from 1995 to 2012.

Based on different ICME and MC catalogs, the parameters of ICMEs and MCs, the annual variation of numbers, ratios, and the parameters of ICMEs and MCs, have been studied by different authors (*e.g.* Cane and Richardson, 2003b; Jian *et al.*, 2006; Richardson and Cane, 2010; Wu and Lepping, 2007, 2008, 2011, 2015; Wu, Lepping, and Gopalswamy, 2006; Lepping, Wu, and Berdichevsky, 2015; Lepping *et al.*, 2006b, 2011; Lepping and Wu, 2007 and references therein). Most of the previous results are obtained from the statistical

analysis of ICMEs or MCs in different periods. The detailed analysis and the comparison of ICMEs in different solar phases and solar cycles are not fully completed. Now, the *Wind* spacecraft has collected *in-situ* observations for more than 20 years, since 1995. Thus, large sample statistical analysis of ICMEs and MCs can be completed using the *Wind* observations.

In this work, we establish an ICME catalog from 1995 to 2015 based on the *in-situ* magnetic field and solar-wind plasma observations from *Wind*. The suprathermal-electron pitch-angle distribution observations from the *Wind* and ACE spacecraft and the proton and electron-flux observations from *Wind* are also included in this work. The method that we used to determine the ICMEs and a brief introduction of the catalogue are given in Section 2. In Section 3 we discuss the variation of the yearly occurrence frequencies of ICMEs. The yearly occurrence frequencies and ratios of MCs and shocks driven by these ICMEs are also discussed in this section. Furthermore, the properties of ICMEs, the comparison between MC and non-MC ejecta, the yearly variations of ICME parameters and their correlation with the sunspot numbers are shown in Section 4. In Section 5, we compare the properties of the ICMEs with and without shocks. In addition, the properties of the shock-sheath regions of these ICMEs and the primary parameters of these shocks are also shown in Section 5. At last, briefly summaries are given in Section 6.

2. ICME Identification and the Catalog

Different signatures were used to identify ICMEs. In this work, the criteria we used were i) enhanced magnetic-field intensity, ii) smoothly changing magnetic-field direction, iii) declining profile of the solar-wind velocity, iv) low proton temperature, v) low proton plasma β, and vi) bidirectional streaming of electrons. A structure is recognized as an ICME when it fits at least three of the criteria listed above, as in Shen *et al.* (2014). Previous results showed that some ICMEs can drive shocks ahead of them. In this work, we used the criteria of an obvious jump in magnetic-field intensity, solar-wind velocity, plasma density, and proton temperature to identify the possible fast upstream shocks ahead of ICMEs. Figure 1 shows an example of the ICME: the 22 – 24 September 1999 event. From 23:24UT 22 September 1999 to 02:33UT 24 September 1999 (the gray shade in Figure 1), the *in-situ* observations show signatures with declining velocity profile, low proton temperature, low plasma β, and bidirectional suprathermal electron streaming. This is an ICME structure that fits at least four of our criteria. About 11 hours earlier, a shock driven by this ICME was detected (the vertical-dashed line in Figure 1). After the shock, the magnetic-field intensity, the solar-wind velocity, the proton number density, and the proton temperature were significantly enhanced. It should be noted that for some events, the boundaries of ICMEs are hard to be determined based on magnetic-field and plasma observations. For these events, energetic-particle intensity depressions are included to check the possible boundaries of ICMEs (*e.g.* Cane and Lario, 2006). Based on these criteria, we clearly identified 465 ICME events from 1995 to 2015, about half (229) of which have upstream shocks. This ratio is consistent with the previous result suggested by Lepping *et al.* (2015) and Wu and Lepping (2016) that 58 % of MCs have upstream shocks.

The magnetic cloud (MC) was thought to be a special type of ICME. Using the MC catalog from Lepping *et al.* (2006a, 2011, 2015), we determined which ICMEs that we obtained in this work are MCs. It should be noted that these catalogs cover the period from 1995 to the end of 2012 only. Thus, for the ICMEs after 2012, we used the following signatures to define the MC: i) enhanced magnetic-field intensity, ii) long and smooth rotation of the magnetic

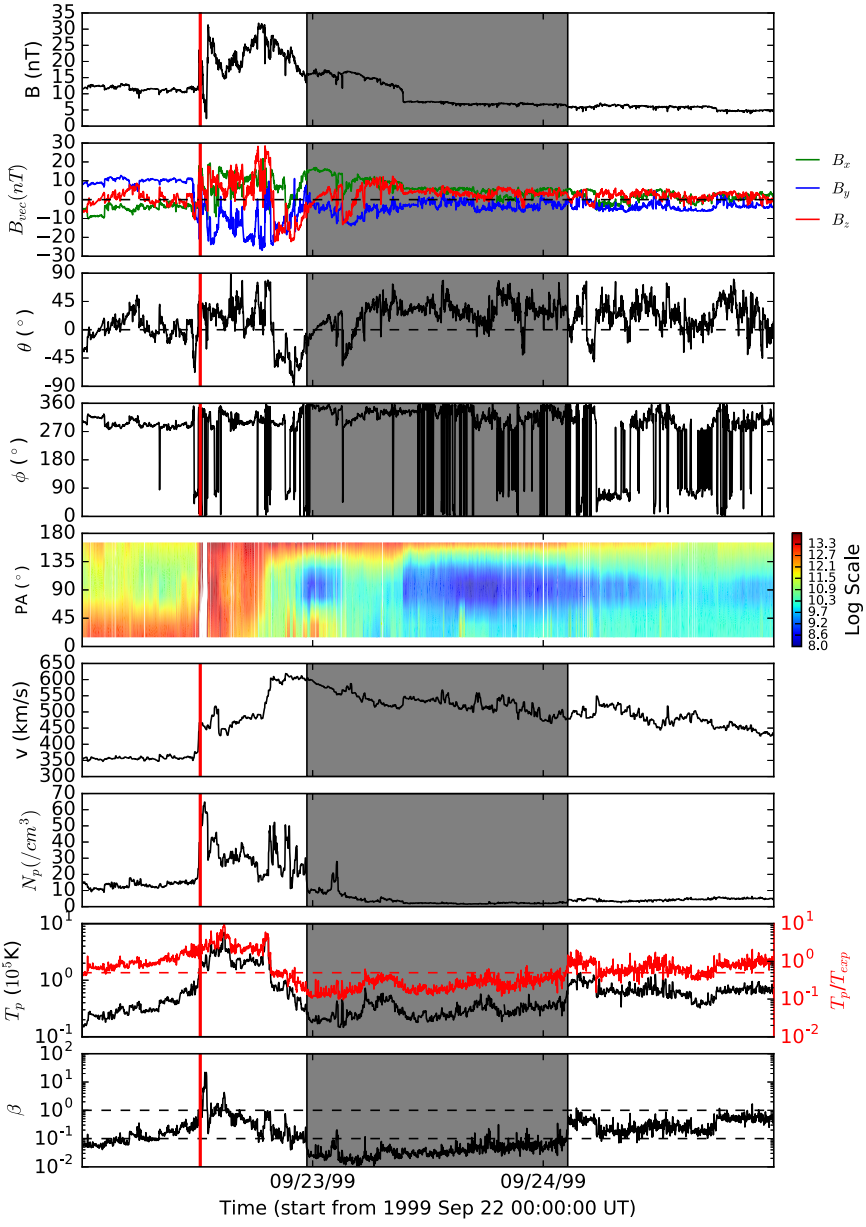

Figure 1 An example of an interplanetary coronal mass ejection (ICME): the 22 – 24 September 1999 event. From top to the bottom, they are the magnetic-field strength [$|B|$], the vector magnetic field in Geocentric Solar Ecliptic (GSE) coordinate system, the elevation [θ] and azimuth [ϕ] of field direction in GSE coordinate system from *Wind*, the suprathermal electron pitch-angle distribution, solar-wind speed [v], proton density [$N_{\rm p}$], proton temperature [$T_{\rm p}$], and the ratio of proton thermal pressure to magnetic pressure [$\beta_{\rm p}$] from *Wind* observations.

List of Interplanetary Coronal Mass Ejections (ICMEs)

No	Shock Time	Start of the Ejecta	End of the Ejecta	MC	Mean Values in the Ejecta							Mean Values in the Sheath Region							Figures
					B (nT)	B_s (nT)	Duration of Bs (hours)	v (km/s)	v_xB_s (mV/m)	T_p (10^5K)	N_p (cm^{-3})	B (nT)	B_s (nT)	Duration of Bs (hours)	v (km/s)	v_xB_s (mV/m)	T_p (10^5K)	N_p (cm^{-3})	
1	-----	1996-05-27T14:44:15	1996-05-28T11:21:25	Y	9.20	4.70	11.70	380.10	1.88	0.25	8.78	------	------	------	------	------	------	------	MAGSWE:EPF
2	-----	1996-07-01T17:15:00	1996-07-02T10:16:29	Y	11.00	4.40	7.70	353.60	1.58	0.31	18.05	------	------	------	------	------	------	------	MAGSWE:EPF
3	-----	1996-08-07T11:42:00	1996-08-08T08:14:59	Y	6.50	2.80	17.20	345.60	0.96	0.30	8.55	------	------	------	------	------	------	------	MAGSWE:EPF
4	-----	1996-12-24T02:53:15	1996-12-24T13:41:15	Y	9.60	-0.00	0.00	377.40	-0.00	0.24	9.06	------	------	------	------	------	------	------	MAGSWE:EPF
5	-----	1996-12-24T16:23:15	1996-12-25T11:24:00	Y	11.00	5.10	6.10	331.70	1.62	0.32	11.75	------	------	------	------	------	------	------	MAGSWE:EPF
6	1997-01-10T00:51:45	1997-01-10T04:41:15	1997-01-11T02:57:45	Y	14.70	7.60	15.70	437.40	3.44	0.26	19.44	8.80	4.50	1.80	440.60	1.99	0.87	13.22	MAGSWE:EPF

Figure 2 A snapshot of the online ICME catalog that is located at http://space.ustc.edu.cn/dreams/wind_icmes/.

field vector, iii) low proton temperature, and low plasma β. A structure that fits all of the above signatures is defined as an MC. These signatures have been widely used to determine MCs from *in-situ* observations (*e.g.* Klein and Burlaga, 1982; Zurbuchen and Richardson, 2006; Zhang *et al.*, 2007). In all, we find that about 35 % (163) ICME events in our list are MCs. This ratio is similar to the results obtained by Gosling (1990), Wu and Lepping (2011) and Richardson and Cane (2010).

An online catalog of these ICMEs is located at http://space.ustc.edu.cn/dreams/wind_icmes/. Figure 2 shows a snapshot of it. The first column in the table shows the order numbers of ICMEs. The second column gives the the arrival times of the shocks driven by these ICMEs. The symbols "—" in this column indicate that no shock driven by these ICMEs could be found. The beginning and the end times of ICMEs are shown in the third and fourth columns. The fifth column gives the results about whether ICMEs are MCs. A letter "Y" indicates that these ICMEs are MCs, while a letter "N" means that these events are not MC (called non-MC ejecta hereafter). The sixth to twelfth columns give the mean values of the magnetic-field intensity [$\langle B \rangle$], the south component of the magnetic field in Geocentric Solar Ecliptic (GSE) [$\langle B_s \rangle$], the duration of B_s [Δt], the solar-wind velocity [$\langle v \rangle$], the dawn–dusk electric field [$\langle vB_s \rangle$], the proton temperature [$\langle T_p \rangle$], and the proton number density [$\langle N_p \rangle$] in the ejecta regions of these ICMEs. The thirteenth to nineteenth columns show these parameters in the shock-sheath regions of these ICMEs. In should be noted that in these columns, these parameters are the mean values during the ejecta regions or the shock sheath regions. If there was no shock driven by a ICME, columns thirteen to nineteen are marked by "—". The magnetic-field and solar-wind plasma images of these ICMEs, as Figure 1 shows, can be obtained at the links in the twentieth column in the online catalog called "MAGSWE". We also provide the electron and proton flux images from *Wind*/3DP in the online catalog at the links of "EPF" in column 20.

Some ICME catalogs are fairly complete. Two of these are i) Richardson and Cane's catalog (RC catalog, Richardson and Cane, 2010), ii) Lan Jian's catalog (JL catalog, Jian *et al.*, 2006). The time period of the RC catalog is from 1996 to 2015. By comparing our list with theirs, we find that a large part of the ICMEs are listed in both catalogs. In the period in common, about 83 % (373) ICMEs in our catalog are listed in RC catalog, but 77 events are only listed in our catalog and 105 events are only listed in the CR catalog. The time period of the JL catalog is from 1995 to 2009. In the period in common from 1995 to 2009, we identified 314 ICME events in total, 75 % (235) of which are listed in the JL catalog. These

results show that there are great similarities between these catalogs, but there are still obvious differences. The main reason is that we use different criteria to identify the ICMEs from *in-situ* observations. As we showed in Section 1, 12 selection criteria can be used to identify the ICME. Only some of them were used to identify ICMEs in different works, however. In our catalog, we mainly consider the magnetic-field intensity, the solar-wind velocity, the proton temperature, the plasma β, and the solar-wind suprathermal electron pitch-angle observations. Different from this, the ion-composition and charge-state observations are taken into consideration in the RC catalog. The ratio of α-particles to protons and the total perpendicular pressure are used in the JL catalog.

3. Yearly Occurrence Frequencies of ICMEs

Panels a and b in Figure 3 show the yearly occurrence frequencies of ICMEs, MCs (blue bars in Panel a) and ICMEs with shocks (red bars in Panel b) from 1995 to 2015. The green diamonds in Panel c show the yearly average sunspot numbers from http://www.sidc.be/silso/home. These panels show that the yearly occurrence frequencies of ICMEs and shocks driven by ICMEs are correlated with the solar-cycle variation. The correlation coefficient between the yearly occurrence frequencies of ICMEs and the sunspot numbers is 0.81, which is similar to previous work (*e.g.* Wu and Lepping, 2011). The correlation coefficient between the yearly occurrence frequencies of the shocks driven by ICMEs and the sunspot numbers is 0.86, which is consistent with a previous study (Wu and Lepping, 2016) for the shocks driven by MCs. The peak yearly occurrence frequency of ICMEs and shocks driven by ICMEs are observed in 2001, with the highest values of 49 and 27, respectively. These correlations can be understood by the fact that the numbers of CMEs and of the fast CMEs that can drive shocks are correlated with the solar-cycle variation (*e.g.* Gopalswamy *et al.*, 2003; Wang and Colaninno, 2014 and references therein). The red-dashed line with solid circles in Panel c shows the ratios of ICMEs that drove shocks [$R_{\rm shock}$] in each year. This panel shows that the ratios of ICMEs driving shocks are correlated with the sunspot numbers. The correlation coefficient between them is 0.65, which is slightly lower than the cc (0.79) for MCs-driven-shock *vs.* SSN (*e.g.* Wu and Lepping, 2016). This indicates that not only the numbers of ICMEs and the shocks driven by them, but also the ratios of ICMEs driving shocks are higher at the solar maximum.

Panels a and c show that the yearly occurrence frequencies of MCs are not correlated with the sunspot numbers. The correlation coefficient between them is only 0.42. This result has been suggested by previous works (*e.g.* Wu, Lepping, and Gopalswamy, 2006; Lepping, Wu, and Berdichevsky, 2015; Lepping *et al.*, 2015). The blue dash–dotted line with squares in Panel c shows the ratios of MCs [$R_{\rm MC}$] in each year. Different from the ratios of the shocks driven by ICMEs, the ratios of MCs do not show a correlation with the sunspot numbers. A high percentage (100 % in 1996) of ICMEs are MCs at solar minimum, but few (less than 20 %) ICMEs are MCs at solar maximum. This also confirms the result that ICMEs are more likely to be MCs at solar minimum (*e.g.* Cane and Richardson, 2003a; Richardson and Cane, 2004, 2010; Jian *et al.*, 2006; Wu and Lepping, 2011, 2015 and references therein). One possible reason is that CMEs are more likely to move to the solar Equator during their propagation in the corona at solar minimum (*e.g.* Cremades and Bothmer, 2004; Wang *et al.*, 2011; Shen *et al.*, 2011; Gui *et al.*, 2011 and references therein). Thus, spacecraft located near the Ecliptic plane are more likely to detect the core regions of CMEs, which are always treated as MCs. In addition, Wu and Lepping (2015) discussed another possibility that the interaction between CMEs and other structures (such as HCS), which would erode

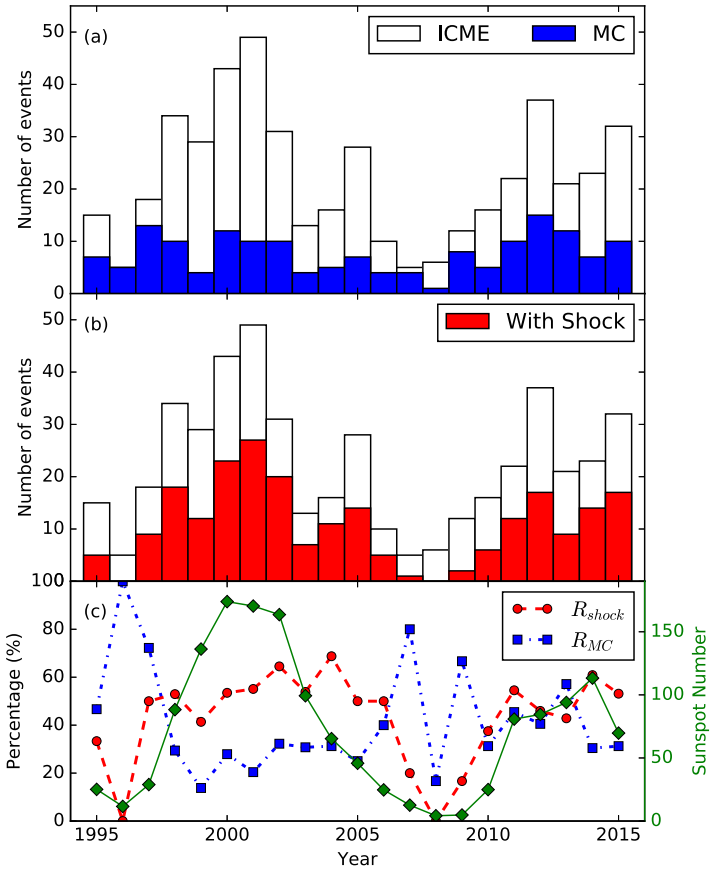

Figure 3 The yearly occurrence frequencies of ICMEs, MCs, and shocks. Panel a shows the yearly occurrence frequencies of ICMEs and MCs (blue). Panel b shows the yearly occurrence frequencies of ICMEs and shocks (red). Panel c shows the ratios of MCs (blue-solid circles) and the ratios of the ICMEs driving shocks (red-solid cycles) varied with time. The dark-green diamonds in Panel c show how the yearly average sunspot numbers varied with time.

the characters of MCs, is rare in solar minimum. Thus, more MCs than non-MC ejecta were observed at solar minimum.

As we discussed in Section 2, there are other well-known ICME or MC lists. Figure 4 shows the comparison between the yearly occurrence frequencies of ICMEs in our catalog and in the RC catalog. The black line with solid circles shows the results based on our catalog, while the red line with squares shows them based on the RC catalog. The blue line with diamonds shows the ICMEs that are listed in both catalogs. It shows that a large fraction of ICMEs are listed in both catalogs. It should be noted that the online version of the RC catalog contains data from 1996 to 2015. For better comparison, we therefore used the ICMEs from these two catalogs during the period from 1996 to 2015 only. During this period, there are 450 ICMEs in our catalog and 478 ICMEs in the RC catalog. 373 ICMEs are overlapping events in these two catalogs. This means that about 83 % ICMEs in our catalog are listed in the RC catalog, while approximately 78 % of their events are contained in our catalog. These comparisons indicate that these two catalogues are similar

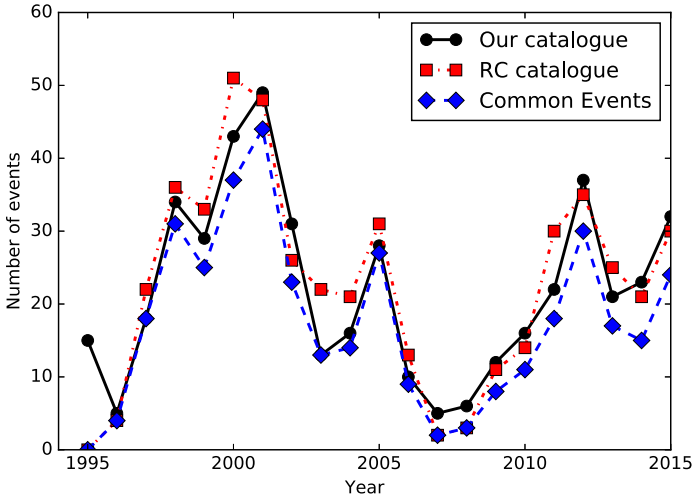

Figure 4 The comparison of the yearly occurrence frequencies of ICMEs between our list with the ICME list of Richardson and Cane (RC list).

but have obvious differences. The reason is that we used different criteria to identify ICMEs, as we discussed in Section 2. In addition, Figure 4 shows that the trend of the numbers that varied with solar cycle is similar. The linear correlation coefficient is 0.93. Some obvious differences exist in these two catalogs. For Solar Cycle 23, the peak of the ICME numbers occurred in 2001 in our catalog, which is consistent with the previous result suggested by Jian *et al.* (2006). But the peak number for the RC list occurred in 2000.

4. Statistical Properties of ICMEs

4.1. Distributions of the Magnetic Field and Plasma Parameters

Figure 5 shows the distributions of the magnetic-field and the solar-wind plasma parameters of the ICME ejecta regions. Panels a – f exhibit the distributions of the mean magnetic-field intensity [$\langle B \rangle$], the mean value of south component of the magnetic field [$\langle B_s \rangle$], the mean solar-wind velocity [$\langle v \rangle$], the mean dawn–dusk electric field [$\langle vB_s \rangle$], the mean proton temperature [$\langle T_p \rangle$], and the mean proton number density [$\langle N_p \rangle$], respectively. As we mentioned in Section 2, in the following analysis, all of the parameters that we used are the mean values in the whole period we considered. In addition, the average values of these parameters for all ICMEs are shown by the arrows at the top of each panel. Based on this figure, we found the following:

i) As shown in Panel a, the magnetic-field intensities of these ICMEs distributed in a wide range, from about 2.84 nT to more than 36.94 nT. The average value for all ICMEs is 10.08 nT, about twice of the background magnetic field (5 nT) at 1 AU. To compare this with the results of Richardson and Cane (2010), we calculated the average value in the same period from 1996 to 2009. During this period, the average magnetic-field intensity of the ICMEs in our catalog is 10.37 nT. This is similar to the average value of ICME (10.1 nT) obtained by Richardson and Cane (2010).

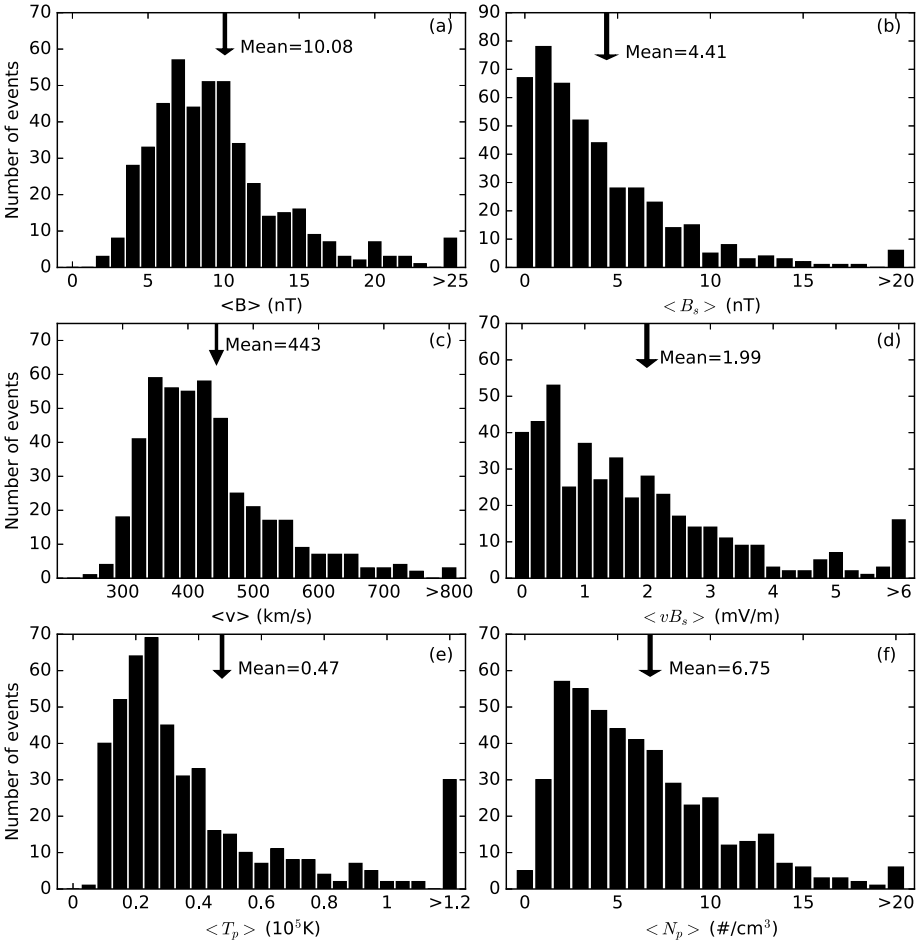

Figure 5 Distributions of the mean values of different parameters of the ejecta regions of ICMEs. Panels a – f show the distributions of $\langle B\rangle$, $\langle B_{\rm s}\rangle$, $\langle v\rangle$, $\langle vB_{\rm s}\rangle$, $\langle T_{\rm p}\rangle$, and $\langle N_{\rm p}\rangle$, respectively. Arrows show the average values for all ICME events.

ii) Velocities of ICMEs concentrate around the value of 400 km s^{-1} as Panel c shown, and, about 77 % of them are located in a narrow range from 300 to 500 km s^{-1}. The average velocity for all ICMEs is 443 km s^{-1}. For the ICMEs from 1996 to 2009, the average values is 458 km s^{-1}, which is similar but slightly lower than the value (476 km s^{-1}) obtained by Richardson and Cane (2010).

iii) The south component of the IMF [$\langle B_{\rm s}\rangle$] and the dawn–dusk electric field [$\langle vB_{\rm s}\rangle$] are important factors in determining the geoeffectiveness of ICMEs (*e.g.* Gonzalez *et al.*, 1994, Wang *et al.*, 2003). Panels b and d show that $\langle B_{\rm s}\rangle$ and $\langle vB_{\rm s}\rangle$ also varied in a wide range. The average and highest values of $\langle B_{\rm s}\rangle$ are 4.40 and 35.39 nT, while the average and highest values of $\langle vB_{\rm s}\rangle$ are 1.99 and 24.22 mV m^{-1}. Previous results showed that the threshold of ICME in causing geomagnetic storms for the mean value of $\langle B_{\rm s}\rangle$ is about 3 nT (Wang *et al.*, 2003). In our list, the $\langle B_{\rm s}\rangle$ in 51 % ICMEs exceed this threshold. This means that about half of the ICMEs might cause geomagnetic storms.

iv) Panels e and f show the distributions of the proton temperature [$\langle T_{\rm p}\rangle$] and the proton number density [$\langle N_{\rm p}\rangle$]. The average values of these two parameters are 0.47×10^5 K and 6.75 cm^{-3}, respectively.

4.2. Comparison between MC and non-MC ejecta

An MC is a special type of ICME. Previous results showed that the magnetic-field intensity in MCs is stronger than in non-MC ejecta (*e.g.* Wu and Lepping, 2011, 2015). Figure 6 shows the distributions of magnetic-field intensities and solar-wind plasma parameters for the ejecta regions of MCs and non-MC ejecta. Similar to previous results, parameters related to the magnetic field [$\langle B\rangle$, $\langle B_{\rm s}\rangle$, and $\langle vB_{\rm s}\rangle$] for the ejecta regions of MCs and non-MC ejecta are significantly different. These parameters in MCs are obviously larger than in non-MC ejecta. Figure 6a shows that the magnetic-field intensity distribution of MCs is obviously

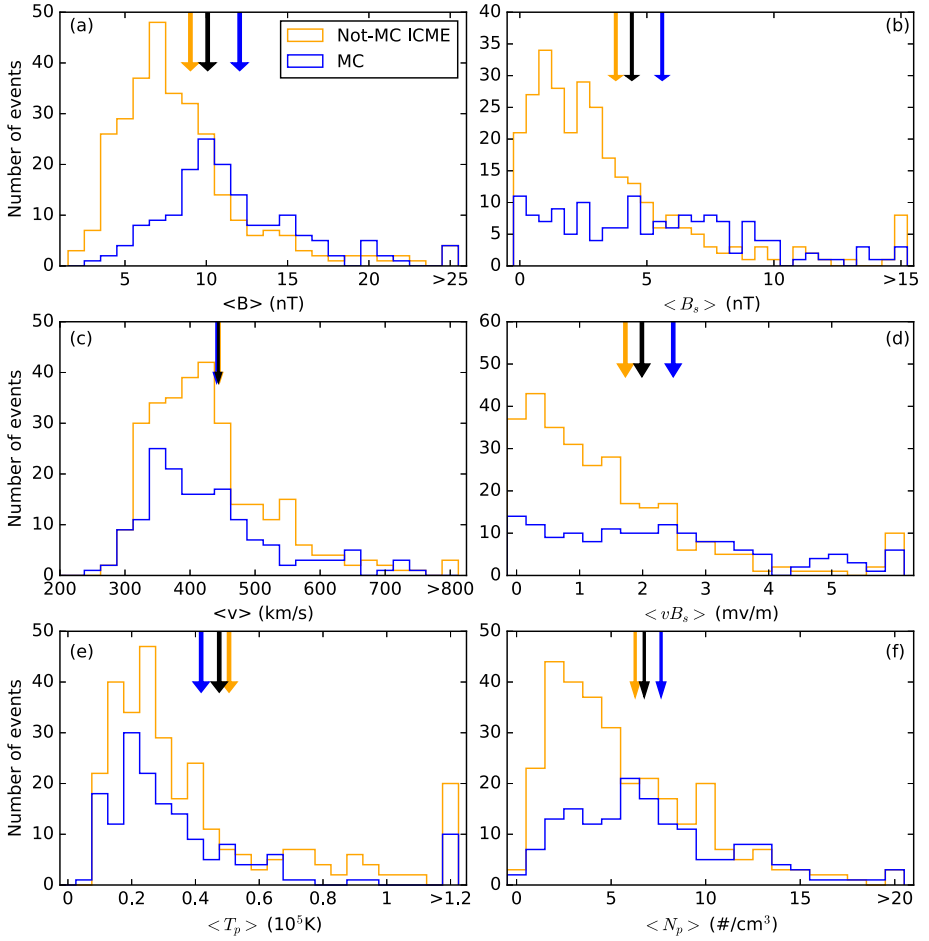

Figure 6 The distributions of the magnetic-field and solar-wind plasma parameters of the ejecta regions of MCs and non-MC ejecta. The black arrows show the average values for all ICMEs. Blue and orange show the MC and non-MC ejecta events, respectively.

right to the distribution of non-MC ejecta. The peak for MC occurred at 10 nT. For non-MC ejecta, it is 7 nT. Averages of $\langle B \rangle$ in MCs and non-MC ejecta are 12.05 and 9.02 nT, respectively. This confirms the previous result that the magnetic field strength in MC is stronger than in non-MC ejecta. In addition, as shown in Panels b and d, the average values of $\langle B_s \rangle$ and $\langle vB_s \rangle$ in MCs are 5.60 nT and 2.49 mV m^{-1}. For non-MC ejecta, they are lower, with average values of 3.78 nT and 1.73 mV m^{-1}. The mean velocity [$\langle v \rangle$] distribution of MCs and non-MC ejecta is shown in Panel c. This shows that the velocities of MCs are slightly lower than non-MC ejecta. The peak of the velocities for MCs is 350 km s^{-1}, while the peak of the non-MC ejecta is 425 km s^{-1}. The average values (441 km s^{-1} for MCs and 445 km s^{-1} for non-MC ejecta) are close to the background solar-wind speed (about 450 km s^{-1}). As shown in Panel e, the proton temperature of MCs is lower than that of non-MC ejecta. The reason may be that the low temperature is a criterion to determine the MC. In addition, Panel f shows that the proton density in MCs is higher than it in non-MC ejecta.

4.3. Solar Cycle Variation of the Magnetic Field and Plasma Parameters

Figure 7 shows the parameters of ICMEs varied with time from 1995 to 2015. Each dot shows an ICME event. The red dots in diamonds show the events with yearly maximum values in each year. Panels a to e show that the maximum values of $\langle B \rangle$, $\langle B_s \rangle$, $\langle v \rangle$, $\langle vB_s \rangle$, and $\langle T_p \rangle$ for ICMEs in each year vary with the solar cycle. At solar maximum, the yearly maximum values of ICMEs are higher, while they are lower at solar minimum. The event with the highest values of $\langle B \rangle$, $\langle B_s \rangle$, and $\langle vB_s \rangle$ from 1995 to 2015 is the MC recorded at 31 March 2001. This event has been studied by Wang, Ye, and Wang (2003). According to Wang, Ye, and Wang (2003), this MC is part of a multiple MC structure. Thus, the strong but short duration magnetic field in this MC might be caused by the interaction (or compression) between multiple MCs during their propagation from the Sun to Earth. The ICME with the highest solar-wind velocity is the 11 – 12 September 2005 event with $\langle v \rangle = 1079$ km s^{-1}.

In addition, the yearly averages of the magnetic field and plasma parameters (green-horizontal lines in Figure 7) also varied with solar cycle. This has also been discussed by Lepping *et al.* (2011). These parameters are higher at solar maximum and lower at solar minimum. Almost all parameters are highest in 2003, which is a few years later than the peak time of the sunspot numbers of Solar Cycle 23. It should be noted that starting in 2008, almost all ICME parameters are smaller than before. This decrease in parameters in ICMEs during this period has also been reported by Jian, Russell, and Luhmann (2011) and Kilpua *et al.* (2012).

5. The ICMEs with shocks

In Section 2 we found that half (229) of the ICMEs have upstream fast-forward shocks. Comparing non-MC ejecta and MCs, we found that MCs are more likely to drive shocks than non-MC ejecta. 61 % of the MCs drove shocks. This is similar to the results obtained by Wu and Lepping (2016). 43 % of the non-MC ejecta drove shocks. The ratio of MCs driving shocks is similar to the previous result that about 56 % of the MCs observed by *Wind* have upstream shocks (Lepping *et al.*, 2015; Wu and Lepping, 2016). As the velocities of fast CMEs can easily exceed the local Alfvén speed and then drive shocks, we can expect that ICMEs with shocks might be faster than the ICMEs without shocks (*e.g.* Gopalswamy, 2006). Figure 8 shows the comparison of the parameters in the ejecta regions between the ICMEs with and without shocks. It is obvious that the distributions of the $\langle B \rangle$,

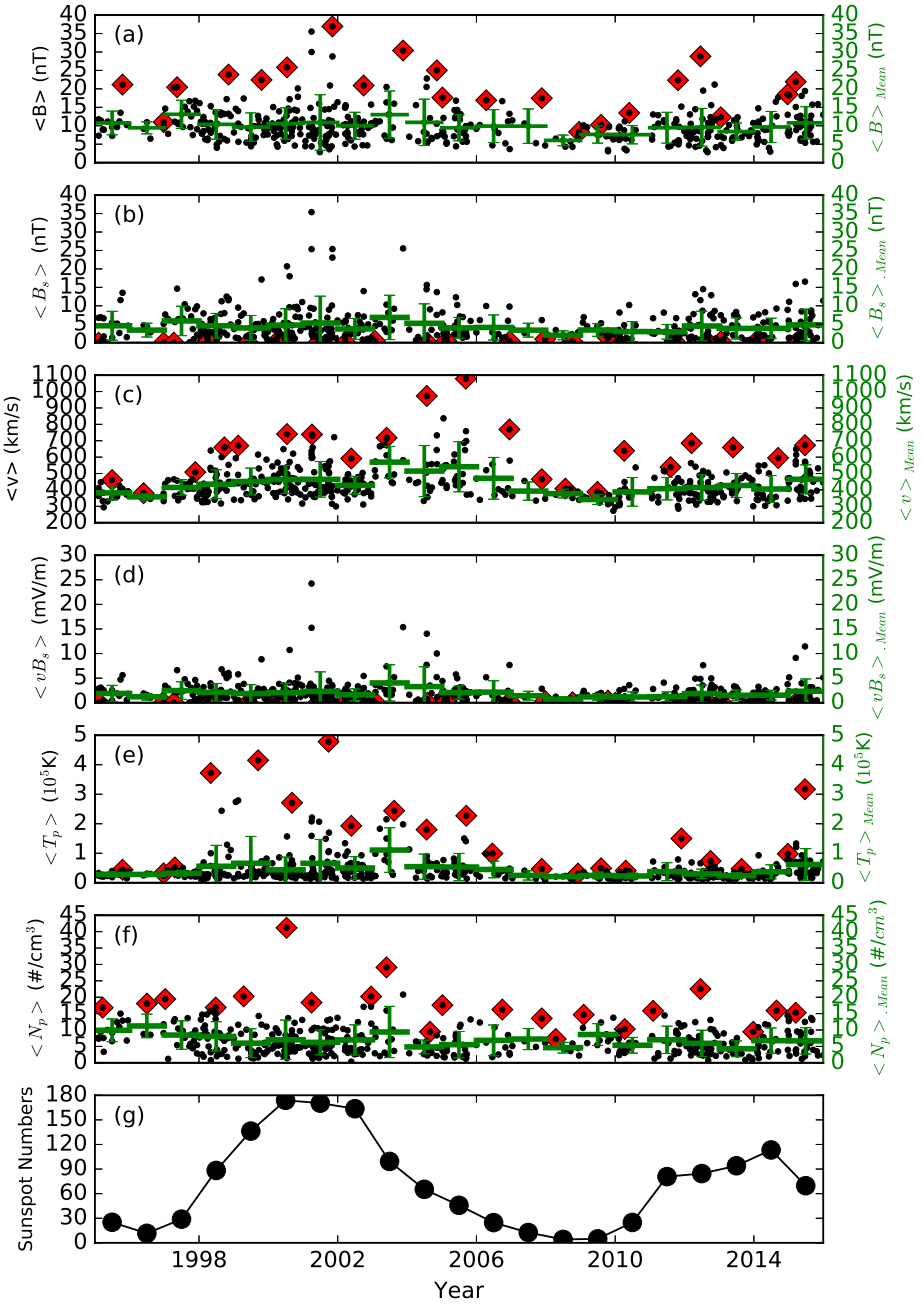

Figure 7 The parameters of the ICME ejecta regions varied with time. Each dot shows an ICME event, and the red dots in diamonds show the events with the maximum value in each year. The green-horizontal lines show the yearly average values of the ejecta regions of ICMEs.

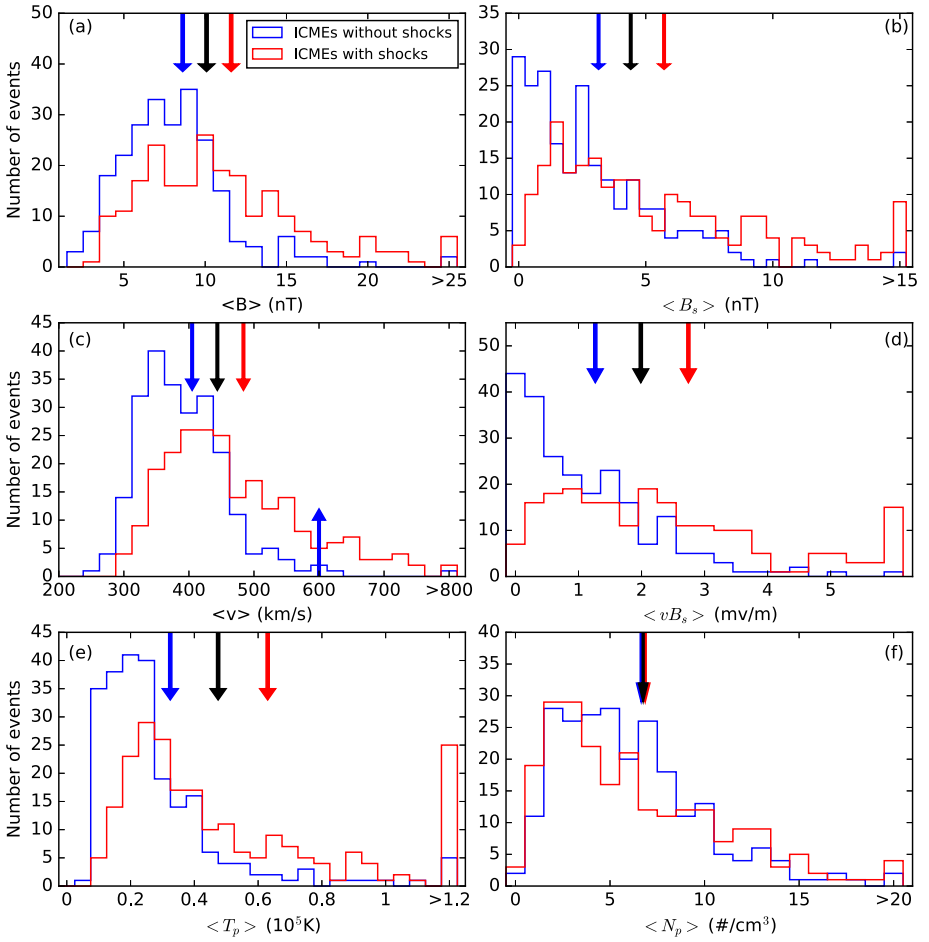

Figure 8 Comparison of the parameters between the ICME ejecta regions with and without shocks. Panels a – f show the distributions of $\langle B \rangle$, $\langle B_s \rangle$, $\langle v \rangle$, $\langle vB_s \rangle$, $\langle T_p \rangle$, and $\langle N_p \rangle$, respectively.

$\langle B_s \rangle$, $\langle v \rangle$, $\langle vB_s \rangle$ and $\langle T_p \rangle$ are different for these two ICMEs types. The ICMEs with shocks are faster than the ICMEs without shocks. Meanwhile, the ICMEs with shocks have a greater magnetic-field strength than the ICMEs without shocks. This difference has also been reported by Gopalswamy (2006) and Wu and Lepping (2016). Figure 8c shows that some of the fast ICMEs did not drive shocks. Conversely, some slow ICMEs drive shocks. One possible reason is the kinematic evolution of ICMEs in interplanetary space, which might cause the ICME velocities to change greatly during their propagation in interplanetary space (*e.g.* Gopalswamy *et al.*, 2000; Lugaz and Kintner, 2012; Vršnak *et al.*, 2013 and references therein). Another possible reason is that the background solar-wind plasma and magnetic-field conditions are different and then the background Alfvén speed might vary in a wide range in different cases. Shen *et al.* (2007) showed two cases in which a fast CME drove a weak shock and a slow CME drove a strong shock near the Sun. They found that this was caused by the different background Alfvén speeds in these two events.

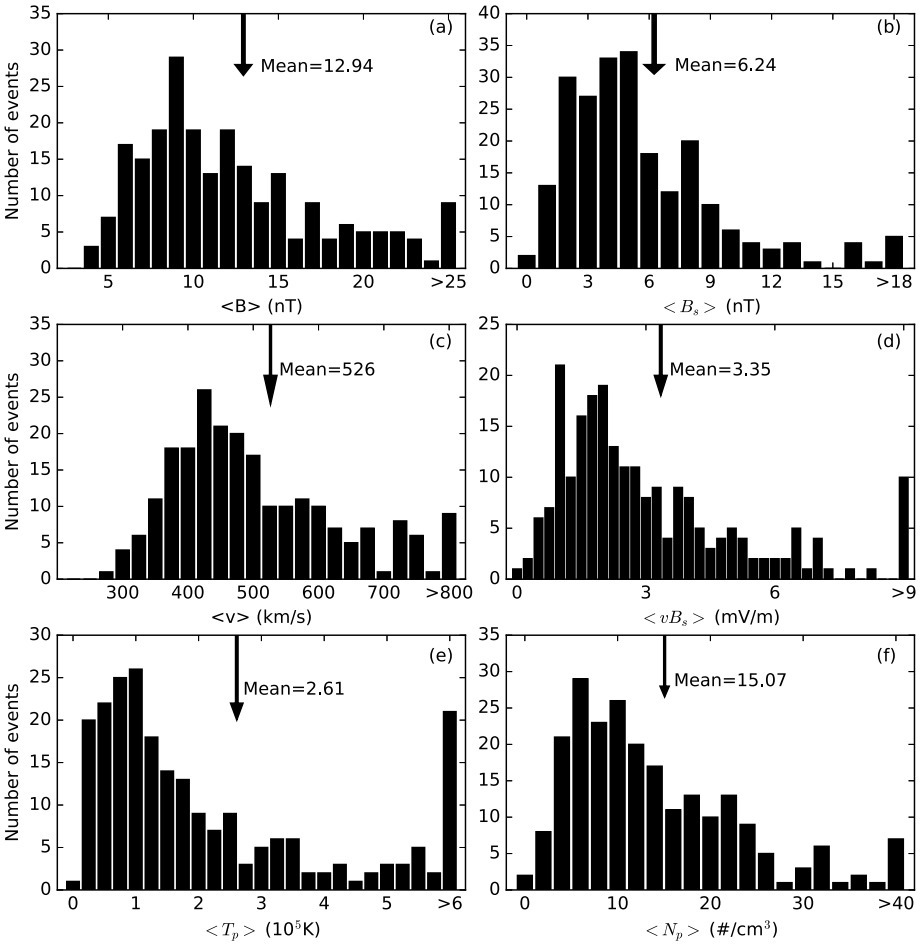

Figure 9 The distributions of different parameters in the shock-sheath regions of these ICMEs. Panels a – f show the distributions of $\langle B \rangle$, $\langle B_s \rangle$, $\langle v \rangle$, $\langle v B_s \rangle$, $\langle T_p \rangle$, and $\langle N_p \rangle$, respectively.

Figure 9 shows the distributions of the magnetic-field and plasma parameters in the shock-sheath regions of these ICMEs. All of these parameters are distributed in a wide range (see Figure 9a – f). The average values for all events of $\langle B \rangle$, $\langle B_s \rangle$, $\langle v \rangle$, $\langle v B_s \rangle$, $\langle T_p \rangle$, and $\langle N_p \rangle$ are 12.94 nT, 6.24 nT, 526 km s^{-1}, 3.35 mV m^{-1}, 2.61 $\times$ 10^5 K and 15.07 cm^{-1}, respectively. All of these values are higher than the values that we obtained in the ejecta region. Compared with the distribution of these parameters in the ejecta region, we found that the distribution of $\langle B_s \rangle$ and $\langle v B_s \rangle$ is clearly different. The peak numbers of $\langle B_s \rangle$ and $\langle v B_s \rangle$ for the ejecta region are located at 1 nT and 0.5 mV m^{-1}. For the sheath region, however, the peaks are located at 5 nT for $\langle B_s \rangle$ and 1 mV, m^{-1} for $\langle v B_s \rangle$. In addition, we also compared the average values of the parameters in the sheath regions of MCs and non-MC ICMEs. It is found that the $\langle B \rangle$, $\langle B_s \rangle$, $\langle v B_s \rangle$, $\langle N_p \rangle$, and $\langle T_p \rangle$ in the sheath regions of MCs (13.81 nT, 6.92 nT, 3.70 mV m^{-1}, 2.66 $\times$ 10^5 K, and 13.96 cm^{-1}) are higher than those in the sheath regions of non-MC ICMEs (12.28 nT, 5.72 nT, 3.08 mV m^{-1}, 2.56 $\times$ 10^5 K, and 13.63 cm^{-1}), which is consistent with the results obtained by Wu and Lepping (2016). The $\langle v \rangle$ in the

sheath region of a MC is 510 km s^{-1}, which is slightly slower than in the sheath region of non-MC ICMEs with the value of 539 km s^{-1}. By checking all ICMEs events with upstream shocks, we found that there are 56 % events in which the magnetic-field intensities in the shock-sheath regions are stronger than those in the ejecta regions. 74 % of the ICMEs have velocities in the shock-sheath regions that are faster than in the ejecta regions. We therefore conclude that the magnetic-field intensities and the velocities in the shock-sheath regions are higher than those in the ejecta regions.

5.1. Shock Parameters

A *Wind* shock list can be found at https://www.cfa.harvard.edu/shocks/publications.html. This has been identified and analyzed by J. Kasper and M. Stevens at the Center for Astrophysics (CfA). We call this shock list the CfA shock list hereafter. This list is updated to April 2014. When we compared our list with the CfA shock list, we found that 76 % of the shocks in our catalog are listed in the CfA shock list during the same period from 1995 to April 2014. Using the shock parameters provided at the CfA website, we discuss the primary shock parameters driven by these ICMEs. The CfA website lists seven groups of shock parameters that have been obtained with different methods. Each group has three main parameters. They are the angle between the shock normal and the upstream magnetic-field directions [θ_{Bn}], the compression ratio, which is defined as the density ratio between the upstream and downstream of shock, and the shock speed along the normal in the spacecraft reference frame. In this work, we used the parameters that we obtained with the RH08 fitting method. The RH08 fitting method is a nonlinear least-squares fitting technique using the magnetohydrodynamic (MHD) Rankine–Hugoniot (RH) conservation equations across the shock (Koval and Szabo, 2008).

By checking the fitting result for the 155 shocks in our list, including the CfA shock parameters, the fitting results of three events are not reliable with negative shock speed and large uncertainties. We therefore removed these events. After this, we have 152 events in the remaining study, 88 of which are (quasi-)perpendicular shocks with $\theta_{Bn} \geq 60°$. This means that 58 % of the shocks driven by ICMEs are (quasi-) perpendicular shocks. 9 % (13) of the shocks driven by ICME are quasi-parallel shocks with $\theta_{Bn} < 30°$. These results are similar to the results obtained for all interplanetary shocks (Berdichevsky *et al.*, 2000).

ICMEs are the drivers of these shocks. We tried to determine the possible correlation between the shock parameters and the ICMEs parameters. This is shown in Figure 10. This figure shows the scatter plots of shock parameters and the ICME mean parameters. The shock speed is an important parameter in determining its geoeffectiveness and particle acceleration ability. To determine the relationship between shock speed and ICME parameters, Panels a and b are shown. The shock speeds (Panel a) might be higher when the ICME is faster with higher mean velocity. The correlation coefficient between them is 0.67. The shock speeds show no correlation with the mean magnetic field strength in ICMEs. The compression ratio can represent the strength of the shock. Panels c and d show that it is not correlated with the ICME parameters.

5.2. The Correlation between Parameters in Ejecta Regions and Shock Sheath Regions

Figure 11 shows the scatter plots of the magnetic-field magnitude, the velocities in the ejecta regions, and the shock-sheath regions. Panel b shows that the mean solar-wind velocities in

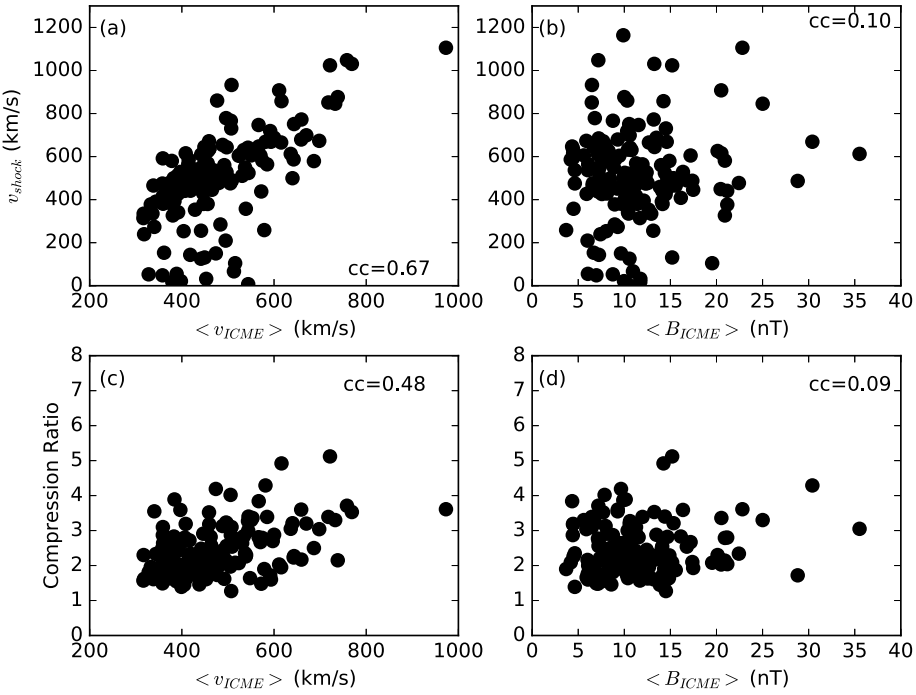

Figure 10 The scatter plots of the primary shock parameters and the ICMEs parameters.

the shock-sheath regions and the ejecta regions are well correlated. The correlation coefficient between them is 0.91. In addition, the average magnetic-field strength in the sheath region and ejecta region show no correlation. No correlations are found between the other parameter groups either.

6. Summary

We have established an ICME catalog for the period from 1995 to 2015. This catalog is mainly based on the magnetic-field and plasma observations from *Wind*. In addition, the suprathermal electron pitch-angle distributions from *Wind* and ACE were used. The proton and electron fluxes observations from *Wind* were also included to determine the possible boundaries of ICMEs. An online version of this catalog can be found at http://space.ustc.edu.cn/dreams/wind_icmes/. Based on this catalog, the yearly occurrence frequencies of ICMEs, the yearly occurrence frequencies and the ratios of MCs and shocks driven by ICMEs, the magnetic-field and solar-wind plasma properties of the ejecta regions and the sheath regions of ICMEs have been discussed. The main results we found are listed below.

i) The yearly occurrence frequencies of ICMEs are correlated well with the sunspot numbers. This confirms the previous results suggested by previous authors (*e.g.* Wu and Lepping (2011) and Richardson and Cane (2010)). In addition, the yearly occurrence frequencies of shocks driven by ICMEs and their ratios of ICMEs are correlated with the sunspot numbers.

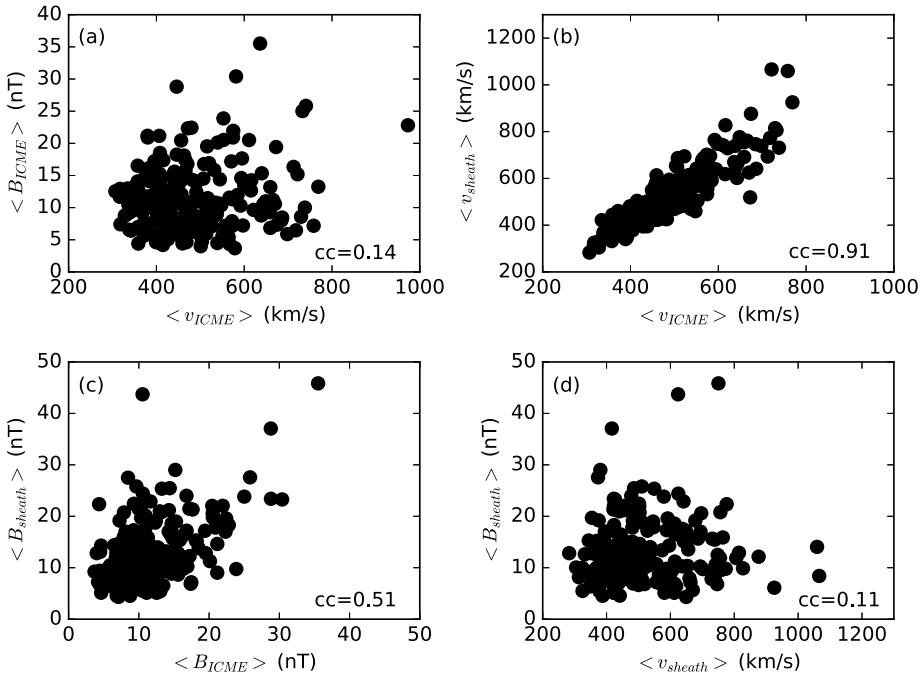

Figure 11 The scatter plots of the mean magnetic field [$\langle B \rangle$] and the mean velocities [$\langle v \rangle$] in the ejecta regions and the shock-sheath regions.

ii) The yearly occurrence frequencies of MCs did not show a correlation with sunspot number. The ratio of MCs to ICMEs is lower at solar maximum and higher at solar minimum. This result confirms the previous result that we can observe MCs with higher possibilities at solar minimum (*e.g.* Wu, Lepping, and Gopalswamy, 2006; Wu and Lepping, 2011, 2015; Lepping *et al.*, 2015 and references therein).

iii) The distributions of the mean magnetic-field and solar-wind plasma parameters [$\langle B \rangle$, $\langle B_s \rangle$, $\langle v \rangle$, $\langle v B_s \rangle$, $\langle T_p \rangle$, and $\langle N_p \rangle$] of ICMEs have been discussed. In addition, by comparing the parameters of MCs with non-MC ejecta, we confirmed the result that the MCs have higher magnetic-field strength than non-MC ejecta (*e.g.* Wu and Lepping, 2011, 2015).

iv) After we discussed the yearly variation of ICME parameters, we found that almost all of these parameters, except for the proton number densities, vary with the solar cycle. The yearly average and maximum values of these parameters after 2008 are lower than those in Solar Cycle 23.

v) About half of the ICMEs drove fast upstream shocks. The ratios of MCs and non-MC ejecta driving shocks are 61 % and 43 %, respectively.

vi) By comparing the parameters of ICMEs with and without shocks, we found that ICMEs with shocks have a faster speed and higher magnetic-field strength than ICMEs without shocks. In addition, the comparison between the parameters in the sheath region and ejecta region for each ICME revealed that magnetic-field intensities and the solar-wind velocities are higher in the shock-sheath regions than those in the ejecta regions of ICMEs.

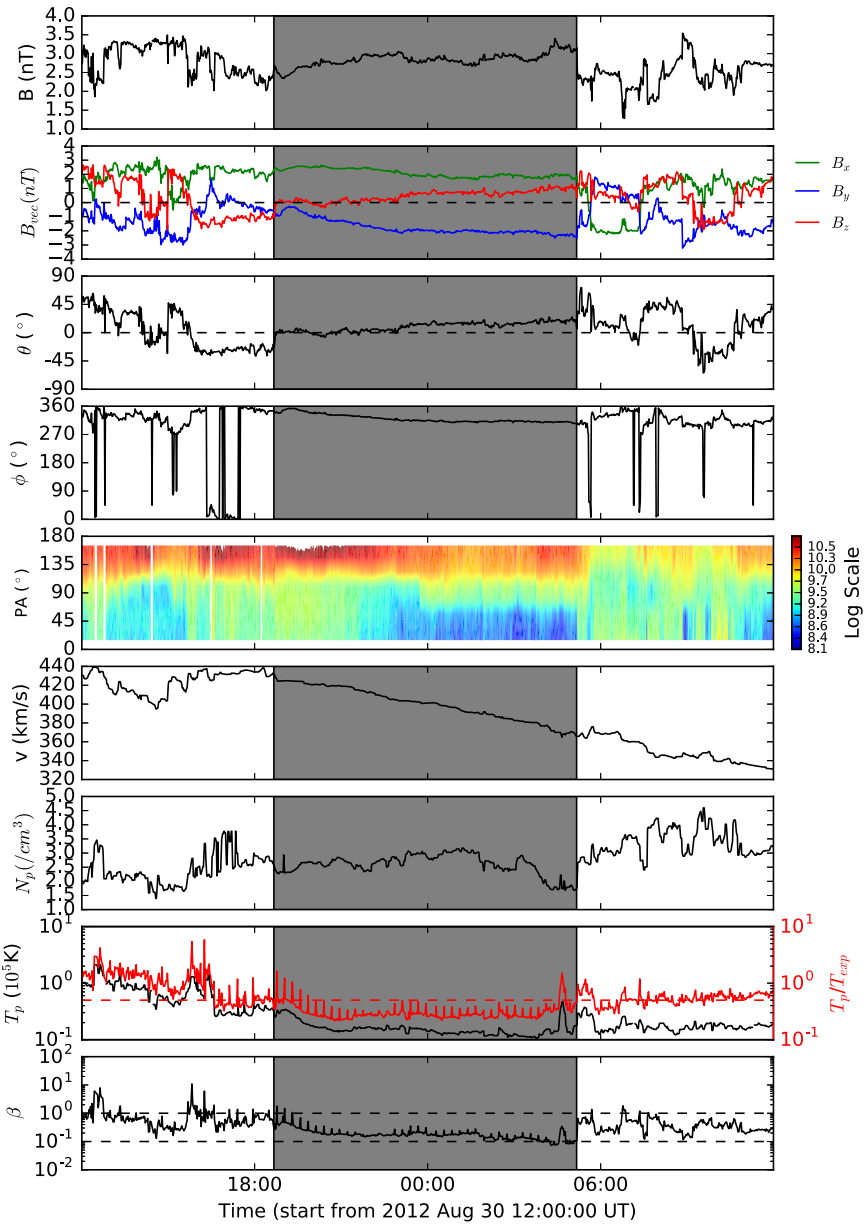

Figure 12 An example of the interplanetary coronal mass ejection (ICME) with lower magnetic-field intensity: the event on 30 August 2012.

It should be noted that the magnetic-field intensity in some events is low. Figure 12 shows an example: the event on 30 August 2012. In this event, the mean IMF intensity [$\langle B \rangle$] is 2.84 nT, which is the lowest in our catalog. Figure 12 shows that this structure clearly fits the following criteria that we used to identify the ICME in this work: i) declining speed profile, ii) lower temperature, iii) lower plasma β, and iv) smoothly rotating magnetic-field vector.

The magnetic field is also stronger than the ambient solar wind because of the very low background magnetic-field intensity. This example shows the possibility that the magnetic field intensity in the background magnetic field can be much lower than 5 nT in some cases. In addition, by checking the RC catalog, the mean magnetic-field strength of 105 (of 478) ICMEs is lower than 6 nT and is lower than 5 nT for 6 events. This confirms the result that the mean magnetic field strength of ICMEs may be small in same cases. The possible reasons are that i) in the criteria we selected in this work, the enhanced magnetic field is only one of six criteria. When a structure fits the other three criteria, it could also be identified as an ICME even though the magnetic field is not strong enough. ii) The background magnetic-field intensity may be lower than 5 nT in some cases.

Acknowledgements We acknowledge the use of the data from *Wind* and ACE spacecraft. We also thank the Harvard-Smithsonian Center for Astrophysics Interplanetary Shock Database (supported by NASA grant number NNX13AI75G) for using their shock parameters. We thank the anonymous referee for the constructive comments. This work is supported by grants from MOST 973 key project (2011CB811403), CAS (Key Research Program KZZD-EW-01 and 100-Talent Program), NSFC (41131065, 41121003, 41274173, 41222031 and 41404134), the fundamental research funds for the central universities and the Specialized Research Fund for State Key Laboratories.

References

Berdichevsky, D.B., Szabo, A., Lepping, R.P., Viñas, A.F., Mariani, F.: 2000, Interplanetary fast shocks and associated drivers observed through the 23rd solar minimum by Wind over its first 2.5 years. *J. Geophys. Res.* **105**(A12), 27289. DOI.

Burlaga, L.F.: 1988, Magnetic clouds and force-free fields with constant alpha. *J. Geophys. Res.* **93**, 7217. ADS.

Burlaga, L., Sittler, E., Mariani, F., Schwenn, R.: 1981, Magnetic loop behind an interplanetary shock – Voyager, Helios, and IMP 8 observations. *J. Geophys. Res. Space Phys.* **86**, 6673. DOI.

Burlaga, L.F., Skoug, R.M., Smith, C.W., Webb, D.F., Zurbuchen, T.H., Reinard, A.: 2001, Fast ejecta during the ascending phase of solar cycle 23: ACE observations, 1998 – 1999. *J. Geophys. Res.* **106**(A), 20957.

Cane, H.V., Lario, D.: 2006, An introduction to CMEs and energetic particles. *Space Sci. Rev.* **123**(1 – 3), 45.

Cane, H.V., Richardson, I.G.: 2003a, Interplanetary coronal mass ejections in the near-Earth solar wind during 1996 – 2002. *J. Geophys. Res. Space Phys.* **108**, 1156. DOI.

Cane, H.V., Richardson, I.G.: 2003b, Interplanetary coronal mass ejections in the near-Earth solar wind during 1996 – 2002. *J. Geophys. Res.* **108**(A), 1156. ADS.

Cane, H.V., Richardson, I.G., Wibberenz, G.: 1997, Helios 1 and 2 observations of particle decreases, ejecta, and magnetic clouds. *J. Geophys. Res.* **102**, 7075. ADS.

Cremades, H., Bothmer, V.: 2004, On the three-dimensional configuration of coronal mass ejections. *Astron. Astrophys.* **422**(1), 307.

Echer, E., Gonzalez, W.D., Tsurutani, B.T.: 2008, Interplanetary conditions leading to superintense geomagnetic storms (Dst < -250 $mboxnT$) during solar cycle 23. *Geophys. Res. Lett.* **35**(6), L06S03.

Gonzalez, W.D., Joselyn, J.A., Kamide, Y., Kroehl, H.W., Rostoker, G., Tsurutani, B.T., Vasyliunas, V.M.: 1994, What is a geomagnetic storm? *J. Geophys. Res.* **99**(A4), 5771.

Gonzalez, W.D., Echer, E., Clua-Gonzalez, A.L., Tsurutani, B.T.: 2007, Interplanetary origin of intense geomagnetic storms (Dst < -100 nT) during solar cycle 23. *Geophys. Res. Lett.* **34**(6), L06101.

Gonzalez, W.D., Echer, E., Tsurutani, B.T., Gonzalez, A.L., Lago, A.: 2011, Interplanetary origin of intense, superintense and extreme geomagnetic storms. *Space Sci. Rev.* **158**(1), 69.

Gopalswamy, N.: 2006, Properties of interplanetary coronal mass ejections. *Space Sci. Rev.* **124**(1), 145.

Gopalswamy, N., Lara, A., Lepping, R.P., Kaiser, M.L., Berdichevsky, D., St Cyr, O.C.: 2000, Interplanetary acceleration of coronal mass ejections. *Geophys. Res. Lett.* **27**, 145. ADS.

Gopalswamy, N., Lara, A., Yashiro, S., Nunes, S., Howard, R.A.: 2003, Coronal mass ejection activity during solar cycle 23. In: Wilson, A. (ed.) *Solar Variability as an Input to the Earth's Environment*, *International Solar Cycle Studies (ISCS)* **SP-535**, ESA, Noordwijk, 403.

Gosling, J.T.: 1990, Coronal mass ejections and magnetic flux ropes in interplanetary space. In: *Physics of magnetic flux ropes (A92-31201 12-75)*, American Geophysical Union, Washington, 343.

Gosling, J.T., Pizzo, V., Bame, S.J.: 1973, Anomalously low proton temperatures in the solar wind following interplanetary shock waves—evidence for magnetic bottles? *J. Geophys. Res.* **78**(13), 2001. DOI.

Gui, B., Shen, C., Wang, Y., Ye, P., Wang, S.: 2011, Quantitative analysis of CME deflections in the corona. *Solar Phys.* **271**, 111.

Hau, L.-N., Sonnerup, B.U.Ö.: 1999, Two-dimensional coherent structures in the magnetopause: Recovery of static equilibria from single-spacecraft data. *J. Geophys. Res. Space Phys.* **104**(A4), 6899. DOI.

Hu, Q., Sonnerup, B.U.Ö.: 2001, Reconstruction of magnetic flux ropes in the solar wind. *Geophys. Res. Lett.* **28**(3), 467.

Hu, Q., Sonnerup, B.U..: 2002, Reconstruction of magnetic clouds in the solar wind: Orientations and configurations. *J. Geophys. Res. Space Phys.* **107**(A7), 1. DOI.

Jian, L.K., Russell, C.T., Luhmann, J.G.: 2011, Comparing solar minimum 23/24 with historical solar wind records at 1 AU. *Solar Phys.* **274**(1 – 2), 321. DOI.

Jian, L., Russell, C.T., Luhmann, J.G., Skoug, R.M.: 2006, Properties of interplanetary coronal mass ejections at one AU during 1995 – 2004. *Solar Phys.* **239**(1-2), 393. DOI.

Kilpua, E.K.J., Liewer, P.C., Farrugia, C., Luhmann, J.G., Möstl, C., Li, Y., Liu, Y., Lynch, B.J., Russell, C.T., Vourlidas, A., Acuna, M.H., Galvin, A.B., Larson, D., Sauvaud, J.A.: 2009, Multispacecraft observations of magnetic clouds and their solar origins between 19 and 23 May 2007. *Solar Phys.* **254**(2), 325.

Kilpua, E.K.J., Jian, L.K., Li, Y., Luhmann, J.G., Russell, C.T.: 2012, Observations of ICMEs and ICME-like solar wind structures from 2007 – 2010 using near-Earth and STEREO observations. *Solar Phys.* **281**(1), 391. DOI.

Kilpua, E.K.J., Mierla, M., Zhukov, A.N., Rodriguez, L., Vourlidas, A., Wood, B.: 2014, Solar sources of interplanetary coronal mass ejections during the solar cycle 23/24 minimum. *Solar Phys.* **289**(10), 3773. DOI.

Klein, L.W.., Burlaga, L.F.: 1982, Interplanetary magnetic clouds at 1 AU. *J. Geophys. Res. Space Phys.* **87**(1), 613.

Koval, A., Szabo, A.: 2008, Modified "Rankine–Hugoniot" shock fitting technique: Simultaneous solution for shock normal and speed. *J. Geophys. Res.* **113**(A10), A10110.

Lepping, R.P., Jones, J.A., Burlaga, L.F.: 1990, Magnetic field structure of interplanetary magnetic clouds at 1 AU. *J. Geophys. Res. Space Phys.* **95**(90), 957.

Lepping, R.P., Wu, C.-C.: 2007, On the variation of interplanetary magnetic cloud type through solar cycle 23: Wind events. *J. Geophys. Res.* **112**(A10), A10103.

Lepping, R.P., Wu, C.-C., Berdichevsky, D.B.: 2015, Yearly comparison of magnetic cloud parameters, sunspot number, and interplanetary quantities for the first 18 years of the wind mission. *Solar Phys.* **290**(2), 553. DOI.

Lepping, R.P., Berdichevsky, D.B., Wu, C.-C., Szabo, A., Narock, T., Mariani, F., Lazarus, a.J., Quivers, a.J.: 2006a, A summary of WIND magnetic clouds for years 1995 – 2003: Model-fitted parameters, associated errors and classifications. *Ann. Geophys.* **24**(1), 215. DOI.

Lepping, R.P., Berdichevsky, D.B., Wu, C.-C., Szabo, A., Narock, T., Mariani, F., Lazarus, a.J., Quivers, a.J.: 2006b, A summary of WIND magnetic clouds for years 1995 – 2003: Model-fitted parameters, associated errors and classifications. *Ann. Geophys.* **24**(1), 215. DOI.

Lepping, R.P., Wu, C.C., Berdichevsky, D.B., Szabo, A.: 2011, Magnetic clouds at/near the 200 – 2009 solar minimum: Frequency of occurrence and some unusual properties. *Solar Phys.* **274**(1 – 2), 345. DOI.

Lepping, R.P., Wu, C.-C., Berdichevsky, D.B., Szabo, A.: 2015, Wind magnetic clouds for 2010 – 2012: Model parameter fittings, associated shock waves, and comparisons to earlier periods. *Solar Phys.* **290**(8), 2265. DOI.

Lugaz, N., Kintner, P.: 2012, Effect of solar wind drag on the determination of the properties of coronal mass ejections from heliospheric images. *Solar Phys.* **285**(1), 281. DOI.

Möstl, C., Temmer, M., Rollett, T., Farrugia, C.J., Liu, Y., Veronig, A.M., Leitner, M., Galvin, A.B., Biernat, H.K.: 2010, STEREO and Wind observations of a fast ICME flank triggering a prolonged geomagnetic storm on 5 – 7 April 2010. *Geophys. Res. Lett.* **37**(2), 24103. ADS.

Richardson, I.G., Cane, H.V.: 2004, The fraction of interplanetary coronal mass ejections that are magnetic clouds: Evidence for a solar cycle variation. *Geophys. Res. Lett.* **31**(18), 8. DOI.

Richardson, I.G., Cane, H.V.: 2010, Near-Earth interplanetary coronal mass ejections during solar cycle 23 (1996 – 2009): Catalog and summary of properties. *Solar Phys.* **264**, 189.

Shen, C., Wang, Y., Ye, P., Zhao, X.P., Gui, B., Wang, S.: 2007, Strength of coronal mass ejection-driven shocks near the sun and their importance in predicting solar energetic particle events. *Astrophys. J.* **670**(1), 849.

Shen, C., Wang, Y., Gui, B., Ye, P., Wang, S.: 2011, Kinematic evolution of a slow CME in corona viewed by STEREO-B on 8 October 2007. *Solar Phys.* **269**(2), 389. ADS.

Shen, C., Wang, Y., Pan, Z., Miao, B., Ye, P., Wang, S.: 1014, Full-halo coronal mass ejections: Arrival at the Earth. *J. Geophys. Res. Space Phys.* **119**(7), 5107. DOI.

Vršnak, B., Žic, T., Vrbanec, D., Temmer, M., Rollett, T., Möstl, C., Veronig, A., Čalogović, J., Dumbović, M., Lulić, S., Moon, Y.-J., Shanmugaraju, A.: 2013, Propagation of interplanetary coronal mass ejections: The drag-based model. *Solar Phys.* **285**(1 – 2), 295. DOI.

Wang, Y.-M., Colaninno, R.: 2014, Is solar cycle 24 producing more coronal mass ejections than cycle 23? *Astrophys. J.* **784**(2), L27. DOI.

Wang, Y.M., Ye, P.Z., Wang, S.: 2003, Multiple magnetic clouds: Several examples during March–April 2001. *J. Geophys. Res. Space Phys.* **108**(A10), 1370. DOI.

Wang, Y.M., Ye, P.Z., Wang, S., Zhou, G.P., Wang, J.X.: 2002, A statistical study on the geoeffectiveness of Earth-directed coronal mass ejections from March 1997 to December 2000. *J. Geophys. Res.* **107**(A11), 1340.

Wang, Y., Shen, C.L., Wang, S., Ye, P.Z.: 2003, An empirical formula relating the geomagnetic storm's intensity to the interplanetary parameters: VBz and Delta t. *Geophys. Res. Lett.* **30**(20), 2039. DOI.

Wang, Y., Chen, C., Gui, B., Shen, C., Ye, P., Wang, S.: 2011, Statistical study of coronal mass ejection source locations: Understanding CMEs viewed in coronagraphs. *J. Geophys. Res.* **116**(A4), A04104.

Wang, Y., Zhou, Z., Shen, C., Liu, R., Wang, S.: 2015, Investigating plasma motion of magnetic clouds at 1 AU through a velocity-modified cylindrical force-free flux rope model. *J. Geophys. Res. Space Phys.* **120**(3), 1543. DOI.

Wimmer-Schweingruber, R.F., Crooker, N.U., Balogh, A., Bothmer, V., Forsyth, R.J., Gazis, P., Gosling, J.T., Horbury, T., Kilchenmann, A., Richardson, I.G., Richardson, J.D., Riley, P., Rodriguez, L., Steiger, R.V., Wurz, P., Zurbuchen, T.H.: 2006, Understanding interplanetary coronal mass ejection signatures. Report of working group B. *Space Sci. Rev.* **123**(1), 177.

Wu, C.-C., Lepping, R.P.: 2007, Comparison of the characteristics of magnetic clouds and magnetic cloud-like structures for the events of 1995 – 2003. *Solar Phys.* **242**(1 – 2), 159.

Wu, C.C., Lepping, R.P.: 2008, Geomagnetic activity associated with magnetic clouds, magnetic cloud-like structures and interplanetary shocks for the period 1995 – 2003. *Adv. Space Res.* **41**(2), 335. DOI.

Wu, C.-C., Lepping, R.P.: 2011, Statistical comparison of magnetic clouds with interplanetary coronal mass ejections for solar Cycle 23. *Solar Phys.* **269**(1), 141. ADS.

Wu, C.-C., Lepping, R.P.: 2015, Comparisons of characteristics of magnetic clouds and cloud-like structures during 1995 – 2012. *Solar Phys.* **290**(4), 1243. DOI.

Wu, C.C., Lepping, R.P.: 2016, Relationships among geomagnetic storms, interplanetary shocks, magnetic clouds, and sunspot number during 1995 – 2012. *Solar Phys.* **291**(1), 265. doi:DOI.

Wu, C.-C., Lepping, R.P., Gopalswamy, N.: 2006, Relationships among magnetic clouds, CMES, and geomagnetic storms. *Solar Phys.* **239**(1), 449.

Wu, C.C., Gopalswamy, N., Lepping, R.P., Yashiro, S.: 2013, Characteristics of magnetic clouds and interplanetary coronal mass ejections which cause intense geomagnetic storms. *Terr. Atmos. Ocean. Sci.* **24**(2), 233. DOI.

Xue, X.H., Wang, Y., Ye, P.Z., Wang, S., Xiong, M.: 2005, Analysis on the interplanetary causes of the great magnetic storms in solar maximum (2000 – 2001). *Planet. Space Sci.* **53**(4), 443. ADS.

Yermolaev, Y.I., Yermolaev, M.Y.: 2006, Statistic study on the geomagnetic storm effectiveness of solar and interplanetary events. *Adv. Space Res.* **37**(6), 1175.

Zhang, J., Richardson, I.G., Webb, D.F., Gopalswamy, N., Huttunen, E., Kasper, J.C., Nitta, N.V., Poomvises, W., Thompson, B.J., Wu, C.-C., Yashiro, S., Zhukov, A.N.: 2007, Solar and interplanetary sources of major geomagnetic storms ($Dst \leq -100$ nT) during 1996 – 2005. *J. Geophys. Res.* **112**(A10), A10102.

Zurbuchen, T.H., Richardson, I.G.: 2006, In-situ solar wind and magnetic field signatures of interplanetary coronal mass ejections. *Space Sci. Rev.* **123**(2006), 31. DOI.